CFSRC COLLOQUIUM

Proceedings of the Cold-Formed Steel Research Consortium Colloquium
20-22 October, 2020 (cfsrc.org)

Impact of Fastener Spacing on the Behavior of Cold-Formed Steel Shear Walls Sheathed with Fiber Cement Board

Fani Derveni[1], Simos Gerasimidis[2], Kara D. Peterman[3]

Abstract

As cold-formed steel (CFS) is progressively used in high seismic regions as part of the designated lateral force resisting system, it is necessary to explore higher capacity systems. Furthermore, these systems must be fully enabled within relevant design specifications. The objective of this work is to provide design guidelines and performance benchmarks for cold-formed steel shear walls sheathed with fiber cement board (FCB). High-fidelity three-dimensional finite element modeling is introduced by investigating wall aspect ratio, and fastener spacing pattern. Herein, fasteners, which represent the critical load path in CFS shear walls, are modelled via experimentally-derived phenomenological models. An experimental program of monotonic and cyclic connection testing is conducted aiming to shed light on the response of cold-formed steel to fiber cement board sheathing connections. Connection backbone parameters are extracted from the experimental results and are implemented in the finite element model. As fastener spacing is decreased, failure mode shifts from fastener-dominant to the steel framing itself. This work aims to characterize this change in limit state and provide recommendations for design. Updates to AISI S400 are proposed, specifically in providing prescriptive design aids for the practicing engineer. Furthermore, the high-fidelity modeling approach expanded upon herein provides an analytical approach to explore the impact of detailing on wall performance. Fiber cement board-sheathed shear walls represent a wealth of design potential in increasing the lateral capacity available in cold-formed steel shear wall systems. This work provides the fundamental behavioral and limit state analysis towards eventual enabling within national specifications.

1. Introduction

Cold-formed steel (CFS) shear walls have been given significant attention due to the numerous benefits they offer as the designated lateral force resisting systems in CFS construction. Economy, structural efficiency, prefabrication and transportation ease are some of the aspects that make CFS an attractive component for research and design. CFS shear walls sheathed with different materials (such as wood, steel, gypsum, cement) or braced by strap are of particular interest in high seismic regions and have been extensively examined through experimental and computational methods in both, small-scale (connections) and full-scale (shear walls) level.

Extensive connection testing between CFS members and sheathing has been conducted to understand the shear connection behavior under monotonic and/or cyclic loading. Oriented strand board (OSB) sheathing was examined by different experimental programs ([1], [2], [3]), providing data for shear connection capacities of different specimen characteristics (i.e. spacing or thickness). Steel sheathing, either steel sheet or corrugated steel sheet has also received experimental attention ([4], [5]) via tests of single-screw specimens. Cement-based and gypsum-based sheathing to CFS connections were also tested ([6], [7]), providing monotonic shear response for various materials and thicknesses.

Shear wall response has been the subject of numerous experimental and modeling efforts to understand behavior, detail impact, and failure modes. OSB-sheathed shear walls of different aspect ratios and wall characteristics were tested under monotonic and cyclic loading ([8], [9], [10]) concluding fastener-governed failure mechanisms between CFS structural frame and OSB sheathing. Steel sheathing is also experimentally examined for steel sheet ([11], [12]) and corrugated steel [13]. Cement-based, gypsum-based, and and/or composite sheathing materials have been increasingly experimentally assessed in single- and/or double-sided walls ([14], [15], [16]) since they offer higher lateral capacities and fire resistance benefits. Different shear wall computational

[1]PhD Candidate, Department of Civil & Environmental Engineering, University of Massachusetts Amherst, fderveni@umass.edu
[2]Assistant Professor, Department of Civil & Environmental Engineering, University of Massachusetts Amherst, sgerasimidis@umass.edu
[3]Assistant Professor, Department of Civil & Environmental Engineering, University of Massachusetts Amherst, kdpeterman@umass.edu

approaches have been conducted through fastener-based modeling. Performance-based models in OpenSees were used for OSB-sheathed walls ([17], [18]), or steel-sheathed walls [19] through Pinching4 connection model. High-fidelity modeling efforts in Ansys were proposed for strap-based walls [20], as well as in Abaqus for OSB ([21], [22], [3]) and steel sheathing [23] providing different methods for connection simulation and response.

This study aims to shed light on the lateral behavior of CFS shear walls sheathed with FCB by investigating the impact of perimeter fastener spacing on strength, stiffness and governing failure modes for these systems. Initially, the shear connection response is experimentally assessed, providing monotonic and cyclic average test data for two different screw types. A fastener-based shear wall finite element modeling approach follows, presenting capacity predictions and governing wall limit states (from fastener failures to CFS member failures) implicit to fastener spacing. The main goal of this work is to provide design predictions for FCB-sheathed shear walls towards an effort of enabling the beneficial lateral behavior of these systems within both, research community and design specifications.

2. Shear connection experimental program

An experimental program composed of in total 12 specimens is conducted herein in order to obtain shear response of cold-formed steel (CFS) to fiber cement board (FCB) connections, and to extract data for shear wall computational modeling. The connections were tested under monotonic and cyclic loading.

The test rig and specimens, as adapted by [3], are illustrated in Figure 1. The specimens are attached to the rig via hot-rolled steel plates at both sides of stud webs in order to provide fixity of the webs against deformation and focus the failure on the connections (exterior plates: 25.4mm (1in.) thick, interior plates: 12.7mm (0.5in.) thick). The top part is subjected to tensile or cyclic loading, while the bottom part is fixed. The specimens are composed of: CFS studs (web: 152.4mm, flange: 41.3mm, lip: 12.7mm, thickness: 1.37mm (600S162-54)), FCB sheathing (length: 304.8mm, width: 406.4mm, thickness: 19.05mm (12in. x 16in. x 3/4in.) and M4 (No. 8) screws (type “a”, type “b”). Two screws are examined herein from which type “a” is used to represent a new screw M4x50, and screw “b” is used to represent a common industrial screw M4x40 (Figure 1c). Two different sheathing screw configurations are examined herein: a) FCB and CFS connected with screw “a” (CFS-a-FCB), and b) FCB and CFS connected with screw “b” (CFS-b-FCB).

Monotonic loading is applied at a rate of 101.6mm/hour (4in./hour) after a pre-loading of 45kN (10lbs). Cyclic loading is applied by defining the commonly used CUREE protocol,

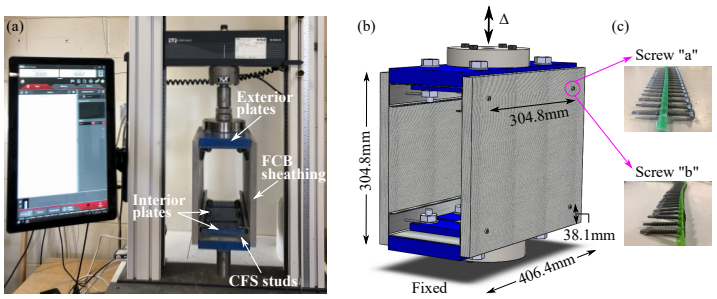

Figure 1: Shear connection test specimens and test rig. (a) Actual photo of test rig in Instron machine, (b) connection specimen schematic, and (c) screw types.

as described by [24]. The resultant cyclic protocol is shown in Figure 2 and it is based on a reference displacement (Δ) defined in Equation 1:

$$\Delta = 0.6\Delta_m \tag{1}$$

where Δ_m is the displacement at 80% of the post-peak load of the prior monotonic tests. The reference displacement Δ of CFS-a-FCB is equal to 7.61mm (0.3in.), while the reference displacement Δ of CFS-b-FCB is equal to 4.59mm (0.2in.).

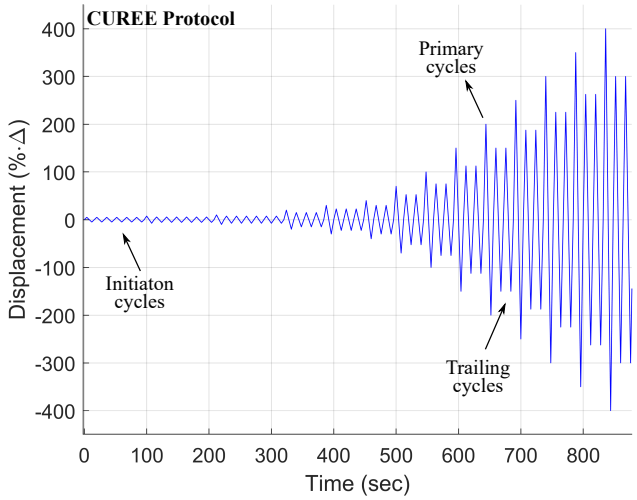

Figure 2: Resultant CUREE protocol for cyclic tests.

3. Experimental results

The test results for the CFS-a-FCB and CFS-b-FCB specimens are depicted in for both monotonic (Figure 3) and cyclic loading (Figure 4). The results show low variability in strength and stiffness for all the repetitions of CFS-a-FCB specimens, while energy dissipation is higher in one of the cyclic repetitions. For the CFS-b-FCB specimens significant strength

variability is illustrated in one of the monotonic repetitions, while strength, stiffness and energy dissipation is consistent within the remaining repetitions. Comparing the average responses between CFS-a-FCB and CFS-b-FCB specimens (shown in Figures 3 and 4 with black lines), a percentage difference of 3.7% and 15% results for monotonic and cyclic tests, respectively. Secant stiffness is higher by 44% and 71% for screw "b" in comparison to screw "a" for monotonic and cyclic tests, respectively.

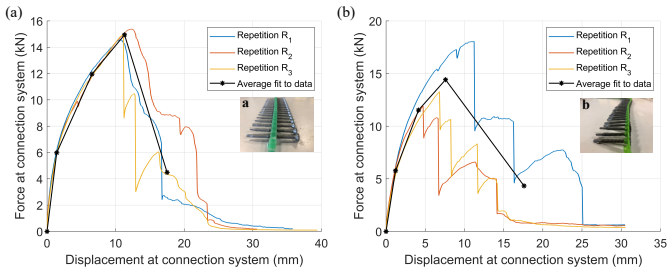

Figure 3: Monotonic experimental results: (a) CFS-a-FCB identical specimens, (b) CFS-b-FCB identical specimens. Average data are extracted (black lines) based on 40%Peak, 80%Peak, 100%Peak, 30%Post-peak load.

The governing failure modes of the different tests are distinguished between shear screw failure or screw pull-through, both followed by screw bearing and/or FCB sheathing edge tear out. Specifically, CFS-a-FCB monotonic repetitions primary failed due to pull-through of the screws accompanied by sheathing edge tear out and shear failure of some of the screws post-peak. For the CFS-b-FCB monotonic repetitions, shear failure of the screws governed the response, followed by screw bearing and/or sheathing edge tear out post-peak. Tilting of the screws at the beginning of the tests occurred at the beginning of all monotonic tests. For all cyclic test repetitions (CFS-a-FCB and CFS-b-FCB), shear screw failure was the primary failure mechanism accompanied by localized bearing in the location of the screws.

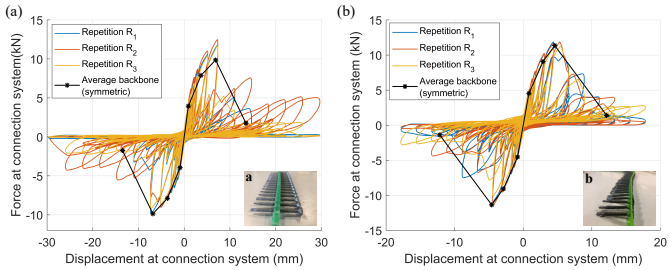

Figure 4: Cyclic experimental results: (a) CFS-a-FCB identical specimens, (b) CFS-b-FCB identical specimens. Symmetric average data (minimum of positive and negative quadrant) are extracted (black lines) based on 40%Peak, 80%Peak, 100%Peak, last point at lower drifts to represent realistic connection behavior.

The response of the system of eight screws is converted to individual screw response via equations introduced by [1]. The force per screw P_i is equal to $P_i = P/4$, the displacement per screw Δ_i is equal to $\Delta_i = \Delta/2$, and the stiffness per screw K_i is equal to $K_i = K/2$, where P, Δ, K are the system force, system displacement, system stiffness respectively. Average individual screw behavior is shown in Table 1.

Table 1: Average backbone parameters for FCB connections

	Average Backbone Parameters			
	Monotonic tests		Cyclic tests	
	FCB-a	FCB-b	FCB-a	FCB-b
Δ_1(mm)/P_1(kN)	0.71 / 1.50	0.60 / 1.44	0.45 / 0.99	0.42 / 1.14
Δ_2(mm)/P_2(kN)	3.28 / 2.99	2.07 / 2.88	1.84 / 1.97	1.45 / 2.27
Δ_3(mm)/P_3(kN)	5.65 / 3.74	3.80 / 3.61	3.43 / 2.47	2.30 / 2.84
Δ_4(mm)/P_4(kN)	8.75 / 1.12	8.80 / 1.08	6.75 / 0.44	6.08 / 0.35

4. Shear wall finite element modeling

The computational method implemented here is a two-stage approach introduced and validated by [3] for OSB-sheathed CFS shear walls and it is expanded herein upon FCB-sheathed shear walls. The two stages are defined as follows:

1. A linear elastic analysis by using a global coordinate system in all CFS-to-FCB connections for calculating angles of axes rotation for all the connections.
2. A pushover analysis by implementing local coordinate systems in all CFS-to-FCB connections for accurately capturing connection response.

The shear wall configuration adopted herein is based on the test rig of McGill University for OSB-sheathed walls [10], as shown in Figure 5a. A wall configuration of 1.22m x 2.44m (4ft x 8ft) is simulated (wall aspect ratio equal to 2) by investigating the impact of different fastener spacings on the lateral performance of the wall. Four different perimeter fastener spacings between CFS and FCB are selected: 152.4mm (6in.), 101.6mm (4in.), 76.2mm (3in.), 50.8mm (2in.), and the different failure modes and limit states are numerically predicted. The wall is constructed of:

- CFS studs (back-to-back chord and field) of a thickness of 1.37mm (54mils), web depth of 92.08mm (3.62in.), flange width of 41.3mm (1.62in.), and lip depth of 12.7mm (0.5in.).
- CFS tracks of a thickness of 1.37mm (54mils), web depth of 92.08mm (3.62in.), and flange width of 30.2mm (1.19in.).
- FCB sheathing of a thickness of 19.05mm (0.75in.)
- M4 x 50 (No. 8) screw (type "a") or M4 x 40 (No.8) screw (type "b") for the connections between CFS members and FCB sheathing.
- Simpson Strong-Tie S/HD10S hold-downs.

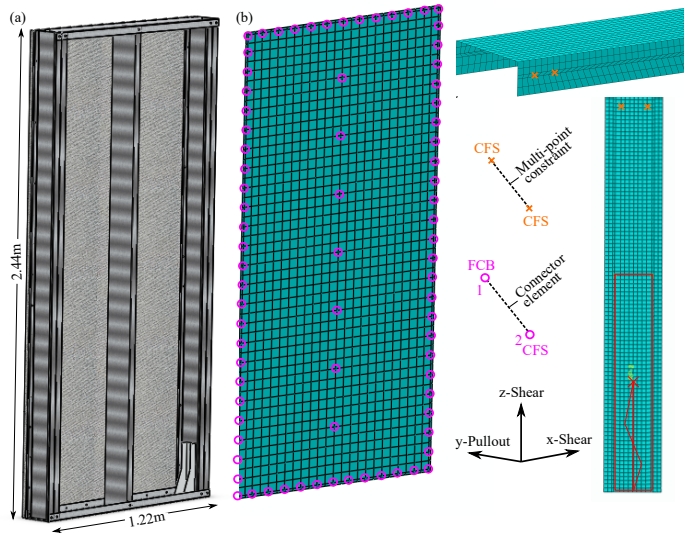

Figure 5: FCB-sheathed CFS shear wall configuration. (a) Schematic representation of the wall. (b) Mesh of all simulated components.

All the simulated components (CFS and FCB) are modeled via S4R shell elements in Abaqus. CFS components are discretized through a finer mesh of 6.35mm (0.25in.) in comparison to FCB sheathing coarse mesh of 50.8mm (2in.). Figure 5b shows the mesh size of the different components.

CFS components (studs and tracks) are simulated through plastic isotropic material properties (Young's modulus: E=203GPa (29500ksi), Yield strength: σ_y=344MPa (50ksi), Poisson's ratio: ν=0.3), while FCB sheathing as elastic isotropic material (Young's modulus: E=8963MPa (1300ksi), Poisson's ratio: ν=0.3).

CFS-to-FCB connections are simulated through connector element Cartesian in Abaqus. Experimental monotonic average data derived by the shear connection testing of the previous section are used to represent the connection response for the two shear directions (Table 1). For the pull-out direction a high stiffness of 1750000kN/m (10000kips/in.) is used to restrain the sheathing out-of-plane movement. Figure 5b indicates the connector element representation between CFS and FCB and a representative coordinate system used herein. CFS-to-CFS connections are modeled via multi-point pinned constraints (MPC pinned) in Abaqus by restraining their translational degrees of freedom. Stud-to-track connections in the center of their flanges and stud-to-stud connections on the webs of chord studs spacing 304.8mm (12in.) are shown in Figure 5b.

At the bottom of the wall, shear anchors and hold-downs are used to restrain the shear wall lateral response. Four shear anchor nodes at the bottom track are used to restrain the horizontal and the out-of-plane (x and y axes) wall direction, while hold-downs are used to prevent the wall uplift through rigid body simulation at the bottom chord-stud webs tied to a reference point and connected to a fixed node via a Spring2 element (Figure 5b). The hold-down in tension carries a stiffness of 22292kN/m (127.3kips/in.) and hold-down in compression carries 1000 times higher the stiffness of the tensile hold-down.

At the top of the wall, the out-of-plane (y axis) wall movement is restrained via a line of six nodes spacing 230mm (9in.) at the top track. Loading is applied at a reference point at the center of the top track rigid body edge through displacement control (displacement of 0.08m (3.15in.) is applied).

5. Finite element modeling results

The computational results of FCB-sheathed walls connected with screw "a" and screw "b" are shown in Figure 6 for the four different examined fastener spacings. Little strength variability exists between the two wall configurations, and specifically peak strength of FCB walls connected with screw "a" is higher within 0.02%-2.5% compared to FCB walls connected with screw "b" for all different spacings. Secant stiffness of FCB walls connected with screw "a" is lower than secant stiffness of FCB walls connected with screw "b" by 12%-21% for all fastener spacings. Furthermore, qualitative results with regards to fastener spacing variation (152.4mm (6in.), 101.6mm (4in.), 76.2mm (3in.), 50.8mm (2in.)) is similar between screw "a" and screw "b" connected walls. The trend in both wall types is that perimeter fastener spacing decrease (more fasteners used in the perimeter) leads to higher wall lateral capacities. However, as fastener spacing decreases to 76.2mm (3in.) and especially to 50.8mm (2in.), the capacity increase is limited in comparison to bigger spacings such as 152.4mm (6in.) and 101.6mm (4in.).

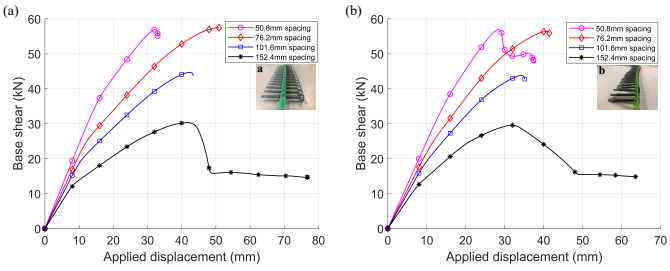

Figure 6: FCB-sheathed CFS shear wall modeling force-displacement results for various fastener spacings: (a) FCB-sheathed walls connected with screw "a", and (b) FCB-sheathed walls fastened with screw "b".

Failure modes of FCB-sheathed shear walls are inherent to fastener spacing and different limit states govern the capacity of these systems. Figure 7 illustrates the two governing failure modes: fastener failures and/or CFS member failures related to the perimeter fastener spacing. In particular, CFS-to-FCB connection failures govern FCB-sheathed wall

response for 152.4mm (6in.) and 101.6mm (4in). The progression of failure is initiated from corner fasteners and it is distributed to adjacent fasteners in the flanges of chord studs and tracks. For 76.2mm (3in.) perimeter spacing, a combination of corner fastener failures and CFS top track yielding and web large deformation occurs. For 50.8mm (2in.) screw spacing, CFS top track yielding and large deformation of the web of the track in the location of the applied load governs the wall response.

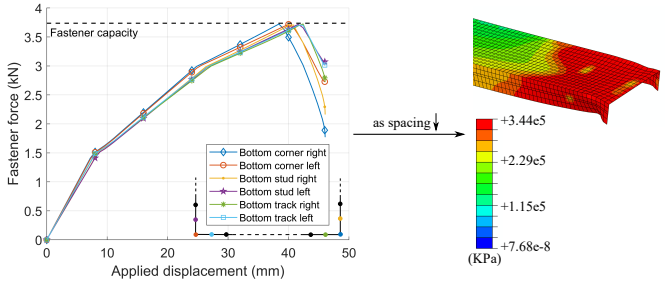

Figure 7: Governing wall limit states: fastener failures or/and CFS track failure (von-Mises stress contours).

6. Shear wall design predictions

Since shear wall design predictions for FCB-sheathed CFS shear walls are not currently available in AISI-S400 predictions, this work constitutes an effort of numerically providing lateral capacities of these higher capacity systems. As shown in Table 2, this work focuses on capacity predictions per unit width (as recommended by AISI code for OSB-sheathed walls) and it provides average predictions (between screw "a" and "b") of FCB-sheathed shear walls for wall aspect ratios of 2. FCB-sheathed shear walls constitute higher capacity systems than the state-of-the-art OSB-sheathed walls available in current AISI-S400 [25].

Table 2: Design predictions for FCB-sheathed CFS shear walls

FCB-sheathed shear walls fastened with M4 screws	Perimeter fastener spacing (mm)	152.4	101.6	76.2	50.8
	Capacity per unit width (kN/m)	24.56	36.30	46.73	46.72

7. Conclusions

This study focused on the performance and limit states of FCB-sheathed CFS shear walls under lateral loading through connection testing and shear wall modeling. The monotonic and cyclic test results between CFS-a-FCB and CFS-b-FCB specimens (screw "a" and "b") resulted to different average response between the two configurations, and specifically 3.7%-15% strength and 45%-70% secant stiffness difference. Screw shear failure or pull-through, both accompanied with FCB edge tear out or/and screw bearing, governed connection response. Monotonic average data were extracted from the tests and used in the shear wall fastener-based modeling approach. The numerical results showed that fastener spacing affected both, wall capacity and governing failure mode. As fastener spacing was reducing (152.4mm (6in.), 101.6mm (4in.), 76.2mm (3in.), 50.8mm (2in.)), more fasteners in the perimeter were used, and higher capacities were predicted. For smaller spacings (such as 76.2mm and 50.8mm) similar shear capacities (1% difference) were predicted due to the different failure mechanisms that governed the response. Failure mode was altered from CFS-to-FCB fastener failures (152.4mm (6in.), 101.6mm (4in.)) to combination of fastener failures and CFS track failure (76.2mm (3in.)) to track failure through yielding and large web deformation (50.8mm (2in.)). Finally, wall capacities per unit width were recommended for researchers and designers for FCB-sheathed higher capacity shear wall systems.

8. Acknowledgments

The authors would like to acknowledge Dr. Benjamin W. Schafer and Dr. Tara C. Hutchinson for the collaborative discussions and advice within CFS-NHERI project. We would also like to thank the CFS-NHERI research group graduate students: Zhidong Zhang, Amanpreet Singh, Hernan Castaneda, and Xiang Wang.

References

[1] L. Vieira and B. W. Schafer, "Experimental results for translational stiffness of stud-sheathing assemblies," *AISI-COFS Project on Sheathing Braced Design of Wall Studs*, 2009.

[2] K. D. Peterman, N. Nakata, and B. W. Schafer, "Hysteretic characterization of cold-formed steel stud-to-sheathing connections," *Journal of Constructional Steel Research*, vol. 101, pp. 254–264, 2014.

[3] F. Derveni, S. Gerasimidis, and K. D. Peterman, "Nonlinear fastener-based modeling of cold-formed steel shear walls," in *Proceedings of the Structures Congress Conference April 5–8. St. Louis, Missouri*, 2020.

[4] F. Tao, A. Chatterjee, and C. D. Moen, "Monotonic and cyclic response of single shear cold-formed steel-to-steel and sheathing-to-steel connections," Virginia Tech., Blacksburg, Virginia, Report. No. CE/VPI-ST-16-01, 2017.

[5] L. Fülöp and D. Dubina, "Design criteria for seam and sheeting-to-framing connections of cold-formed steel shear panels," *Journal of Structural Engineering*, vol. 132, no. 4, pp. 582–590, 2006.

[6] L. Fiorino, T. Pali, B. Bucciero, V. Macillo, M. T. Terracciano, and R. Landolfo, "Experimental study on screwed connections for sheathed cfs structures with

gypsum or cement based panels," *Thin-Walled Structures*, vol. 116, pp. 234–249, 2017.

[7] S. Selvaraj and M. Madhavan, "Investigation on sheathing-fastener connection failures in cold-formed steel wall panels," in *Structures*, Elsevier, vol. 20, 2019, pp. 176–188.

[8] R. L. Serrette, J. Encalada, M. Juadines, and H. Nguyen, "Static racking behavior of plywood, osb, gypsum, and fiberbond walls with metal framing," *Journal of Structural Engineering*, vol. 123, no. 8, pp. 1079–1086, 1997.

[9] P. Liu, K. D. Peterman, and B. W. Schafer, "Impact of construction details on osb-sheathed cold-formed steel framed shear walls," *Journal of Constructional Steel Research*, vol. 101, pp. 114–123, 2014.

[10] A. E. Branston, C. Y. Chen, F. A. Boudreault, and C. A. Rogers, "Testing of light-gauge steel-frame - wood structural panel shear walls.," *Canadian Journal of Civil Engineering*, vol. 33, no. 5, pp. 561–572, 2006, ISSN: 03151468.

[11] C. Yu, H. Vora, T. Dainard, J. Tucker, and P. Veetvkuri, "Steel sheet sheathing options for cold-formed steel framed shear wall assemblies providing shear resistance," University of North Texas, Denton, Texas, USA, Report. No. UNT-G76234, 2007.

[12] J. DaBreo, N. Balh, C. Ong-Tone, and C. Rogers, "Steel sheathed cold-formed steel framed shear walls subjected to lateral and gravity loading," *Thin-Walled Structures*, vol. 74, pp. 232–245, 2014.

[13] L. Fülöp and D. Dubina, "Performance of wall-stud cold-formed shear panels under monotonic and cyclic loading: Part i: Experimental research," *Thin-Walled Structures*, vol. 42, no. 2, pp. 321–338, 2004.

[14] S. Mohebbi, S. R. Mirghaderi, F. Farahbod, A. B. Sabbagh, and S. Torabian, "Experiments on seismic behaviour of steel sheathed cold-formed steel shear walls cladded by gypsum and fiber cement boards," *Thin-Walled Structures*, vol. 104, pp. 238–247, 2016.

[15] M. S. Hoehler, C. M. Smith, T. C. Hutchinson, X. Wang, B. J. Meacham, and P. Kamath, "Behavior of steel-sheathed shear walls subjected to seismic and fire loads," *Fire safety journal*, vol. 91, pp. 524–531, 2017.

[16] M. Zeynalian and H. R. Ronagh, "Seismic performance of cold formed steel walls sheathed by fibre-cement board panels," *Journal of Constructional Steel Research*, vol. 107, pp. 1–11, 2015.

[17] S. Buonopane, G. Bian, T. Tun, and B. Schafer, "Computationally efficient fastener-based models of cold-formed steel shear walls with wood sheathing," *Journal of Constructional Steel Research*, vol. 110, pp. 137–148, 2015.

[18] S. Kechidi and N. Bourahla, "Deteriorating hysteresis model for cold-formed steel shear wall panel based on its physical and mechanical characteristics," *Thin-Walled Structures*, vol. 98, pp. 421–430, 2016.

[19] A. Singh and T. C. Hutchinson, "Finite element modeling and validation of steel-sheathed cold-formed steel framed shear walls," in *Proceedings of the International Specialty Conference on Cold-Formed Steel Structures. St. Louis, Missouri*, 2018.

[20] M. Zeynalian and H. R. Ronagh, "A numerical study on seismic performance of strap-braced cold-formed steel shear walls," *Thin-walled structures*, vol. 60, pp. 229–238, 2012.

[21] H. H. Ngo, "Numerical and experimental studies of wood sheathed cold-formed steel framed shear walls," M.S. thesis, Johns Hopkins University, Baltimore, MD, 2014.

[22] C. Ding, "Monotonic and cyclic simulation of screw-fastened connections for cold-formed steel framing," M.S. thesis, Virginia Tech, Blacksburg, VA, 2015.

[23] Z. Zhang and B. W. Schafer, "Simulation of steel sheet sheathed cold-formed steel framed shear walls," in *Proceedings of the Annual Proceedings of the Annual Stability Conference Structural Stability Research Council April 2–5. St. Louis, Missouri*, 2019.

[24] H. Krawinkler, F. Parisi, L. Ibarra, A. Ayoub, and R. Medina, "Development of a testing protocol for wood frame structures, curee publication no," *W-02, California*, 2000.

[25] AISI-S400-15, "North american standard for seismic design of cold-formed steel structural systems," in *AISI-S400*, Washington, D.C.: American Iron and Steel Institute, 2015.